
Perceptual Adversarial Robustness: Defense Against Unseen Threat Models

Cassidy Laidlaw
University of Maryland
claidlaw@umd.edu

Sahil Singla
University of Maryland
ssingla@cs.umd.edu

Soheil Feizi
University of Maryland
sfeizi@cs.umd.edu

Abstract

We present adversarial attacks and defenses for the perceptual adversarial threat model: the set of all perturbations to natural images which can mislead a classifier but are imperceptible to human eyes. The perceptual threat model is broad and encompasses L_2 , L_∞ , spatial, and many other existing adversarial threat models. However, it is difficult to determine if an arbitrary perturbation is imperceptible without humans in the loop. To solve this issue, we propose to use a *neural perceptual distance*, an approximation of the true perceptual distance between images using internal activations of neural networks. In particular, we use the Learned Perceptual Image Patch Similarity (LPIPS) distance. We then propose the *neural perceptual threat model* that includes adversarial examples with a bounded neural perceptual distance to natural images. Under the neural perceptual threat model, we develop two novel perceptual adversarial attacks to find any imperceptible perturbations to images which can fool a classifier. Through an extensive perceptual study, we show that the LPIPS distance correlates well with human judgements of perceptibility of adversarial examples, validating our threat model. Because the LPIPS threat model is very broad, we find that Perceptual Adversarial Training (PAT) against a perceptual attack gives robustness against many other types of adversarial attacks. We test PAT on CIFAR-10 and ImageNet-100 against 12 types of adversarial attacks and find that, for each attack, PAT achieves close to the accuracy of adversarial training against just that perturbation type. That is, PAT generalizes well to unforeseen perturbation types. This is vital in sensitive applications where a particular threat model cannot be assumed, and to the best of our knowledge, PAT is the first adversarial defense with this property.

1 Introduction

Many modern machine learning algorithms are susceptible to adversarial examples: carefully crafted inputs designed to fool models into giving incorrect outputs [1, 2, 3, 4]. For instance, an imperceptible change to each pixel in an image of a dog could cause a classifier to predict its label as cat. Adversarial examples are serious concerns in safety-critical applications of machine learning, such as self-driving cars. Thus, much research has focused on increasing classifiers’ robustness against adversarial attacks [5, 6, 7].

Existing adversarial defenses for image classifiers generally consider simple threat models. An adversarial threat model defines a set of perturbations that may be made to an image in order to produce an adversarial example. Common threat models include the L_2 and L_∞ threat models, which constrain adversarial examples to be close to the original image in L_2 or L_∞ distances. Some work has proposed additional threat models which allow spatial perturbations [8, 9, 10], recoloring [11, 12, 13], and other modifications [14, 15] of an image.

There are multiple issues with these unrealistically constrained adversarial threat models. First,

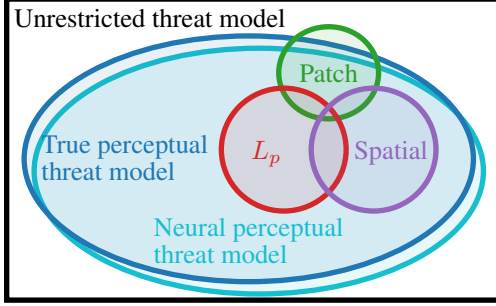


Figure 1: Relationships between various adversarial threat models. L_p and spatial adversarial attacks are contained within the perceptual threat model, while patch attacks may be perceptible and thus are not entirely contained. In this paper, we propose the *neural perceptual threat model* that is based on an approximation of the true perceptual distance using neural networks. In particular, we use the LPIPS distance [22] in our attack and defense methods.

hardening against one threat model assumes that an adversary will only attempt attacks within that threat model. Although a classifier may be trained to be robust against L_∞ attacks, for instance, an attacker could easily generate a spatial attack to fool the classifier. One possible solution is to train against multiple threat models simultaneously [16, 12, 17]. However, this generally results in a lower robustness against any one of the threat models when compared to hardening against that threat model alone. Furthermore, not all possible threat models may be known at the training time, and adversarial defenses do not usually generalize well to unforeseen threat models [18].

The ideal solution to these drawbacks would be a defense that is robust against a wide, unconstrained threat model. We differentiate between two such threat models. The *unrestricted adversarial threat model* [19] encompasses any adversarial example that is labeled as one class by a classifier but a different class by humans. On the other hand, we define the *perceptual adversarial threat model* as including all perturbations of natural images such that the perturbations are imperceptible to a human. Most existing narrow threat models such as L_2 , L_∞ , etc. are subsets of the perceptual threat model (Figure 1). Some other threat models, such as adversarial patch attacks [20], may include perceptible changes without changing the true class of an image and as such are contained in the unrestricted adversarial threat model. In this work, we focus on the perceptual threat model.

The perceptual threat model can be formalized given the true perceptual distance $d^*(\mathbf{x}_1, \mathbf{x}_2)$ between images \mathbf{x}_1 and \mathbf{x}_2 , defined as how different two images appear to humans. For some threshold ϵ^* , which we call the perceptibility threshold, images \mathbf{x} and \mathbf{x}' are indistinguishable from one another as long as $d^*(\mathbf{x}, \mathbf{x}') \leq \epsilon^*$. Note that in general ϵ^* may depend on the specific input. Then, the perceptual threat model for a natural input \mathbf{x} includes all adversarial examples $\tilde{\mathbf{x}}$ which cause misclassification but are imperceptibly different from \mathbf{x} , i.e. $d^*(\mathbf{x}, \tilde{\mathbf{x}}) \leq \epsilon^*$.

The true perceptual distance $d^*(\cdot, \cdot)$, however, cannot be easily computed or optimized against. To solve this issue, we propose to use a *neural perceptual distance*, an approximation of the true perceptual distance between images using neural networks. Fortunately, there have been many surrogate perceptual distances proposed in the computer vision literature such as SSIM [21]. Recently, Zhang et al. [22] discovered that comparing the internal activations of a convolutional neural network when two different images are passed through provides a measure, LPIPS, that correlates well with human perception. We propose to use the LPIPS distance $d(\cdot, \cdot)$ in place of the true perceptual distance $d^*(\cdot, \cdot)$ to formalize the *neural perceptual threat model*.

We present adversarial attacks and defenses for the neural (LPIPS) perceptual threat model. Generating adversarial examples bounded by the LPIPS distance is difficult compared to generating L_p adversarial examples because of the complexity and non-convexness of the constraint. However, we solve a simplified case with a linear approximation of the classification network and a quadratic approximation of the LPIPS distance using the conjugate gradient method. Repeatedly applying this step yields an iterative attack called **Perceptual Projected Gradient Descent (PPGD)**. We also form a Lagrangian relaxation of the constrained optimization problem of finding a perceptual adversarial example; this leads to an attack, **Lagrangian Perceptual Attack (LPA)**, similar to that of Carlini and Wagner [23]. In addition to these attacks, which are suitable for evaluation of a classifier against the perceptual threat model, we also develop Fast-LPA, a more efficient version of LPA that we use in **Perceptual Adversarial Training (PAT)**.

Remarkably, using PAT to train a neural network classifier produces a single model with close to state-of-the-art robustness against a variety of imperceptible perturbations, including L_∞ , L_2 , L_1 , spatial, recoloring, and JPEG attacks on CIFAR-10 and ImageNet-100 (a subset of ImageNet) (Tables

2 and 3). For example, PAT achieves 68% and 73% accuracies against spatial [10] and recoloring [12] attacks, respectively, while threat-specific adversarial training (AT) [6] methods achieve 76% and 81% accuracies. In contrast, AT against L_2 achieves only 15% and 60% accuracies against these attacks, respectively. PAT also leads to high Unforeseen Attack Robustness (UAR) [18], a measure of how well an adversarial defense generalizes to threat models that it was not trained against.

Does the LPIPS distance accurately reflect human perception when it is used to evaluate adversarial examples? We performed a study on Amazon Mechanical Turk (AMT) to determine how perceptible 14 different types of adversarial perturbations such as L_∞ , L_2 , spatial, and recoloring attacks are at multiple threat-specific bounds. We find that LPIPS correlates well with human judgements across different adversarial perturbation types we examine. This indicates that our LPIPS-based threat model closely matches the true perceptual threat model and reinforces the utility of our perceptual attacks to measure adversarial robustness against an expansive threat model. Furthermore, this study allows calibration of a variety of attack bounds to a single perceptibility metric. We will release our dataset of adversarial examples along with the annotations made by participants for further study.

2 Related Work

Adversarial robustness Adversarial robustness has been studied extensively for L_2 or L_∞ threat models [5, 23, 6] and non- L_p threat models such as spatial perturbations [8, 10, 9], recoloring of an image [11, 12, 13], and perturbations in the frequency domain (JPEG attacks) [18]. The most popular known adversarial defense for these threat models is adversarial training [24, 25, 26] where a neural network is trained to minimize the worst-case loss in a region around the input. Recent evaluation methodologies such as Unforeseen Attack Robustness (UAR) [18] and the Unrestricted Adversarial Examples challenge [19] have raised the problem of finding an adversarial defense which gives good robustness under more general threat models. Sharif et al. [27] conduct a perceptual study showing that L_p threat models are a poor approximation of the perceptual threat model. Dunn et al. [28] and Xu et al. [29] have developed adversarial attacks that manipulate higher-level, semantic features. Jordan et al. [16] first explored quantifying adversarial distortions with LPIPS distance.

Perceptual similarity Two basic similarity measures for images are the L_2 distance and the Peak Signal-to-Noise Ratio (PSNR). However, these similarity measures disagree with human vision on many types of perturbations such as blurring and spatial transformations, which has motivated others such as SSIM [21], MS-SSIM [30], CW-SSIM [31], HDR-VDP-2 [32] and LPIPS [22].

3 Neural Perceptual Threat Model

Since the true perceptual distance between images cannot be efficiently computed, we use approximations of it using neural networks, i.e. neural perceptual distances. In this paper, we focus on the LPIPS distance [22] while we note that other neural perceptual distances can also be used in our attacks and defenses.

Let $g : \mathcal{X} \rightarrow \mathcal{Y}$ be a convolutional image classifier network defined on images $\mathbf{x} \in \mathcal{X}$. Let g have L layers, and let the internal activations (outputs) of the l -th layer of $g(\mathbf{x})$ for an input \mathbf{x} be denoted as $g_l(\mathbf{x})$. Zhang et al. [22] have found that normalizing and then comparing the internal activations of convolutional neural networks correlates well with human similarity judgements. Thus, the first step in calculating the LPIPS distance using the network $g(\cdot)$ is to normalize the internal activations across the channel dimension such that the L_2 norm over channels at each pixel is one. Let $\hat{g}_l(\mathbf{x})$ denote these channel-normalized activations at the l -th layer of the network. Next, the activations are normalized again by layer size and flattened into a single vector $\phi(\mathbf{x})$, defined as:

$$\phi(\mathbf{x}) \triangleq \left(\frac{\hat{g}_1(\mathbf{x})}{\sqrt{w_1 h_1}}, \dots, \frac{\hat{g}_L(\mathbf{x})}{\sqrt{w_L h_L}} \right),$$

where w_l and h_l are the width and height of the activations in layer l , respectively. The function $\phi : \mathcal{X} \rightarrow \mathcal{A}$ thus maps the inputs $\mathbf{x} \in \mathcal{X}$ of the classifier $g(\cdot)$ to the resulting normalized, flattened internal activations $\phi(\mathbf{x}) \in \mathcal{A}$, where $\mathcal{A} \subseteq \mathbb{R}^m$ refers to the space of all possible resulting activations. The LPIPS distance $d(\mathbf{x}_1, \mathbf{x}_2)$ between images \mathbf{x}_1 and \mathbf{x}_2 is then defined as:

$$d(\mathbf{x}_1, \mathbf{x}_2) \triangleq \|\phi(\mathbf{x}_1) - \phi(\mathbf{x}_2)\|_2. \quad (1)$$

Now let $f : \mathcal{X} \rightarrow \mathcal{Y}$ be a classifier which maps inputs $\mathbf{x} \in \mathcal{X}$ to labels $f(\mathbf{x}) \in \mathcal{Y}$. $f(\cdot)$ could be the

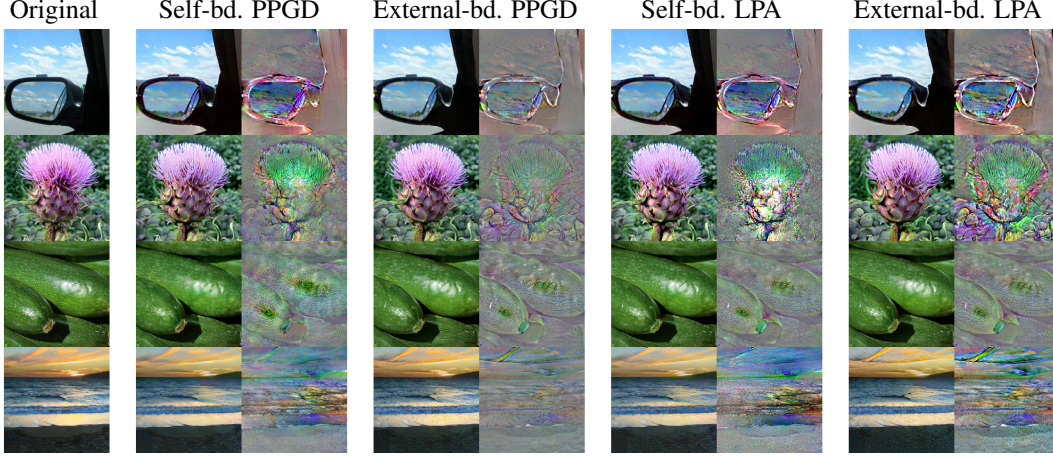


Figure 2: Adversarial examples generated using self-bounded and externally-bounded PPGD and LPA perceptual adversarial attacks (Section 4) with a large bound. Original images are shown in the left column and magnified differences from the original are shown to the right of the examples.

same as $g(\cdot)$, or it could be a different network; we experiment with both. For a given natural input \mathbf{x} with the true label y , a neural (LPIPS) perceptual adversarial example with a perceptibility bound ϵ is an input $\tilde{\mathbf{x}} \in \mathcal{X}$ such that two conditions hold:

$$f(\tilde{\mathbf{x}}) \neq y \quad \text{and} \quad d(\mathbf{x}, \tilde{\mathbf{x}}) = \|\phi(\mathbf{x}) - \phi(\tilde{\mathbf{x}})\|_2 \leq \epsilon. \quad (2)$$

That is, $\tilde{\mathbf{x}}$ must be perceptually similar to \mathbf{x} but cause f to misclassify.

4 Perceptual Adversarial Attacks

We propose attack methods which attempt to find an adversarial example with small perceptual distortion. Developing adversarial attacks that utilize the proposed neural perceptual threat model is more difficult than that of standard L_p threat models, because the LPIPS distance constraint is more complex than L_p constraints. In general, we find an adversarial example that satisfies (2) by maximizing a loss function \mathcal{L} within the LPIPS bound. The loss function we use is similar to the margin loss from Carlini and Wagner [23], defined as

$$\mathcal{L}(f(\mathbf{x}), y) \triangleq \min \left(\kappa, \left(\max_{i \neq y} z_i(\mathbf{x}) \right) - z_y(\mathbf{x}) \right),$$

where $z_i(\mathbf{x})$ is the i -th logit output of the classifier $f(\cdot)$. $\kappa \geq 0$ defines the “confidence” of the misclassification; we use $\kappa = 1$. This gives the constrained optimization problem

$$\max_{\tilde{\mathbf{x}}} \mathcal{L}(f(\tilde{\mathbf{x}}), y) \quad \text{subject to} \quad d(\mathbf{x}, \tilde{\mathbf{x}}) = \|\phi(\mathbf{x}) - \phi(\tilde{\mathbf{x}})\|_2 \leq \epsilon. \quad (3)$$

Note that in this attack problem, the classifier network $f(\cdot)$ and the LPIPS network $g(\cdot)$ are fixed. These two networks could be identical, in which case the same network that is being attacked is used to calculate the LPIPS distance that bounds the attack; we call this a *self-bounded* attack. If a different network is used to calculate the LPIPS bound, we call it an *externally-bounded* attack.

Based on this formulation, we propose two perceptual attack methods, Perceptual Projected Gradient Descent (PPGD) and Lagrangian Perceptual Attack (LPA). See Figure 2 for sample results.

Perceptual Projected Gradient Descent (PPGD) The first of our two attacks is analogous to the PGD [6] or FGSM^k [5] attacks used for L_p threat models. In general, these attacks consist of iteratively performing two steps on the current adversarial example candidate: (a) taking a step of a certain size under the given distance that maximizes a first-order approximation of the misclassification loss, and (b) projecting back onto the feasible set of the threat model.

Identifying the ideal first-order step is easy in L_2 and L_∞ threat models; it is the gradient of the loss function and the sign of the gradient, respectively. However, computing this step is not straightforward with the LPIPS distance, because the distance metric itself is defined by a neural network. Following (3), we desire to find a step δ to maximize $\mathcal{L}(f(\mathbf{x} + \delta), y)$ such that $d(\mathbf{x} + \delta, \mathbf{x}) =$

$\|\phi(\mathbf{x} + \delta) - \phi(\mathbf{x})\|_2 \leq \eta$, where η is the step size. Let $\hat{f}(\mathbf{x}) := \mathcal{L}(f(\mathbf{x}), y)$ for an input $\mathbf{x} \in \mathcal{X}$. Let J be the Jacobian of $\phi(\cdot)$ at \mathbf{x} and $\nabla \hat{f}$ be the gradient of $\hat{f}(\cdot)$ at \mathbf{x} . Then, we can approximate (3) using a first-order Taylor's approximation of ϕ and \hat{f} as follows:

$$\max_{\delta} \quad \hat{f}(\mathbf{x}) + (\nabla \hat{f})^\top \delta \quad \text{subject to} \quad \|J\delta\|_2 \leq \eta. \quad (4)$$

We show that this constrained optimization can be solved in a closed form:

Lemma 1. *Let J^+ denote the pseudoinverse of J . Then the solution to (4) is given by*

$$\delta^* = \eta \frac{(J^\top J)^{-1}(\nabla \hat{f})}{\|(J^+)^\top(\nabla \hat{f})\|_2}.$$

See Appendix A.1 for the proof. This solution is still difficult to efficiently compute, since calculating J^+ and inverting $J^\top J$ are computationally expensive. Thus, we approximately solve for δ^* using the conjugate gradient method; see Appendix A.1 for details.

Perceptual PGD consists of repeatedly finding first-order optimal δ^* to add to the current adversarial example $\tilde{\mathbf{x}}$ for a number of steps. Following each step, if the current adversarial example $\tilde{\mathbf{x}}$ is outside the LPIPS bound, we project $\tilde{\mathbf{x}}$ back onto the threat model such that $d(\tilde{\mathbf{x}}, \mathbf{x}) \leq \epsilon$. The exact projection is again difficult due to the non-convexity of the feasible set. Thus, we use an approximate projection as follows: Let $\delta = \tilde{\mathbf{x}} - \mathbf{x}$. We use the bisection root finding method (see Algorithm 4 in the appendix) to find $\alpha \in [0, 1]$ such that $d(\mathbf{x} + \alpha\delta, \mathbf{x}) - \epsilon = 0$. Then, we project $\tilde{\mathbf{x}}$ to $\mathbf{x} + \alpha\delta$.

Lagrangian Perceptual Attack (LPA) The second of our two attacks uses a Lagrangian relaxation of the attack problem (3) similar to that used by Carlini and Wagner [23] for constructing L_2 and L_∞ adversarial examples. We call this attack the Lagrangian Perceptual Attack (LPA) because we perform a search for the optimal Lagrangian weight λ to apply to the constraint. To derive the attack, we use the following Lagrangian relaxation of (3):

$$\max_{\tilde{\mathbf{x}}} \quad \mathcal{L}(f(\tilde{\mathbf{x}}), y) - \lambda \max \left(0, \|\phi(\tilde{\mathbf{x}}) - \phi(\mathbf{x})\|_2 - \epsilon \right). \quad (5)$$

The perceptual constraint cost, multiplied by λ in (5), is designed to be 0 as long as the adversarial example is within the allowed perceptual distance; i.e. $d(\tilde{\mathbf{x}}, \mathbf{x}) \leq \epsilon$; once $d(\tilde{\mathbf{x}}, \mathbf{x}) > \epsilon$, however, it increases linearly by the LPIPS distance from the original input \mathbf{x} .

Similar to L_p attacks of Carlini and Wagner [23], we adaptively change λ to find an adversarial example within the allowed perceptual distance. In particular, we start with a small value of λ (i.e. $\lambda = 10^{-2}$) and optimize (5) using a variant of gradient descent with decreasing step size η . After this step, if $d(\mathbf{x}, \tilde{\mathbf{x}}) > \epsilon$, we increase λ by a factor of 10 and repeat the optimization. We repeat this for up to 5 iterations. Finally, we project the resulting adversarial example $\tilde{\mathbf{x}}$ into the threat model using the same algorithm used in PPGD (see Appendix A.2 for details).

5 Perceptual Adversarial Training

LPIPS attacks can be used to harden a classifier against the perceptual threat model. The intuition, which we verify in Section 7, is that if a model is robust against LPIPS attacks, it can demonstrate an enhanced robustness against other types of unforeseen adversarial attacks such as StAdv [10] or ReColorAdv [12]. Inspired by adversarial training used to robustify models against L_p attacks, we propose a method called Perceptual Adversarial Training (PAT). PAT utilizes perceptual adversarial attacks to increase the classifier's robustness against not only LPIPS-specific attacks, but also a wide range of other threat models.

Suppose we wish to train a classifier $f(\cdot)$ over a distribution of inputs and labels $(\mathbf{x}, y) \sim \mathcal{D}$ such that it is robust to the perceptual threat model with bound ϵ . Let \mathcal{L}_{ce} denote the cross entropy (negative log likelihood) loss and suppose the classifier $f(\cdot)$ is parameterized by θ_f . Then, PAT consists of optimizing $f(\cdot)$ in a manner analogous to L_p adversarial training [6]:

$$\min_{\theta_f} \mathbb{E}_{(\mathbf{x}, y) \sim \mathcal{D}} \left[\max_{d(\tilde{\mathbf{x}}, \mathbf{x}) \leq \epsilon} \mathcal{L}_{ce}(f(\tilde{\mathbf{x}}), y) \right]. \quad (6)$$

The training formulation attempts to minimize the worst-case loss within a neighborhood of each training point \mathbf{x} . In PAT, the neighborhood is bounded by the LPIPS distance. Recall that the LPIPS distance is itself defined based on a particular neural network classifier. We refer to the normalized,

Table 1: Correlation between the perceptibility of attacks and various distance measures: L_2 , SSIM [21], and LPIPS [22] calculated using various architectures [34, 35, 36] trained normally and with adversarial training (AT).

Arch. Training	L_2	SSIM	AlexNet	VGG-16	ResNet-50				
			Normal	Normal	Normal	AT L_∞	AT L_2	PAT	PAT-AlexNet
Correl. (r)	0.58	0.68	0.85	0.81	0.84	0.70	0.66	0.62	0.61

flattened activations of the network used to define LPIPS as $\phi(\cdot)$ and θ_ϕ to refer to its parameters. We explore two variants of PAT differentiated by the choice of the network used to define $\phi(\cdot)$. In *externally-bounded* PAT, a separate, pretrained network is used to calculate $\phi(\cdot)$ the LPIPS distance $d(\cdot, \cdot)$. In *self-bounded* PAT, the same network which is being trained for classification is used to calculate the LPIPS distance, i.e. $\theta_\phi \subseteq \theta_f$. Note that in self-bounded PAT the definition of the LPIPS distance changes during the training as the classifier is optimized.

The inner maximization in (6) is intractable to compute exactly. However, we can use the perceptual attacks developed in Section 4 to approximately solve it. Since the inner maximization must be solved repeatedly during the training process, we use a variant of the LPA attack called Fast-LPA. Fast-LPA is inexpensive compared to LPA because it does not search for an ideal λ value; see Appendix A.3 and Algorithm 3 for details. The resulting adversarial examples are given to the classifier $f(\cdot)$ and its parameters are updated by stochastic gradient descent (SGD):

$$\min_{\theta_f} \mathbb{E}_{(\mathbf{x}, y) \sim \mathcal{D}} \left[\mathcal{L}_{\text{ce}} \left(f(\text{FastLPA}(f, d, \mathbf{x}, y, \epsilon)), y \right) \right].$$

Training a classifier with PAT gives robustness against a wide range of adversarial threat models (see Section 7). However, it tends to give low accuracy against natural, unperturbed inputs. Thus, we use a technique from Balaji et al. [33] to improve natural accuracy in PAT-trained models: at each training step, only inputs which are classified correctly without any perturbation are attacked. In addition to increasing natural accuracy, this also improves the speed of PAT since only some inputs from each batch must be attacked.

6 Perceptual Evaluation

We conduct a thorough perceptual evaluation of our LPIPS-based threat model and attacks to ensure that the resulting adversarial examples are imperceptible. We also compare the perceptibility of LPIPS-based attacks to 12 narrow threat models: spatially transformed adversarial examples (StAdv) [10], functional adversarial attacks (ReColorAdv) [12], and the 10 UAR attacks [18], which include L_∞ , L_2 , JPEG (frequency domain), and other threat models. The comparison allows us to determine if the LPIPS distance is a good surrogate for human comparisons of similarity. It also allows us to set bounds across threat models with approximately the same level of perceptibility.

To determine how perceptible a particular threat model is at a particular bound (e.g. L_∞ attacks at $\epsilon = 8/255$), we follow a procedure from Xiao et al. [10]. We show pairs of images to participants on Amazon Mechanical Turk (AMT), an online crowdsourcing platform. In each pair, one image is a natural image from ImageNet-100 and one image is an adversarial perturbation of the natural image, generated using the particular attack against a classifier hardened to that attack. The images are shown for 2 seconds, after which the participant must choose which image they believe is the original, unmodified one. We report the proportion of pairs for which participants are correct as the *perceptibility* of the attack. For a completely imperceptible attack, perceptibility is 50%, since participants must guess at each pair randomly; for a completely perceptible attack, perceptibility is 100%, since participants will always know which image is natural.

We collect about 1,000 annotations of image pairs for each of 3 bounds for all 12 threat models, plus our PPGD and LPA attacks (37k annotations total for 7.4k image pairs). The three bounds for each attack are labeled as small, medium, and large; bounds with the same label have similar perceptibility across threat models (see Appendix C Table 4). We will make the dataset of image pairs and associated annotations available for use by the community.

To determine if the LPIPS threat model is a good surrogate for the perceptual threat model, we use various classifiers to calculate the LPIPS distance $d(\cdot, \cdot)$ between the pairs of images used in the

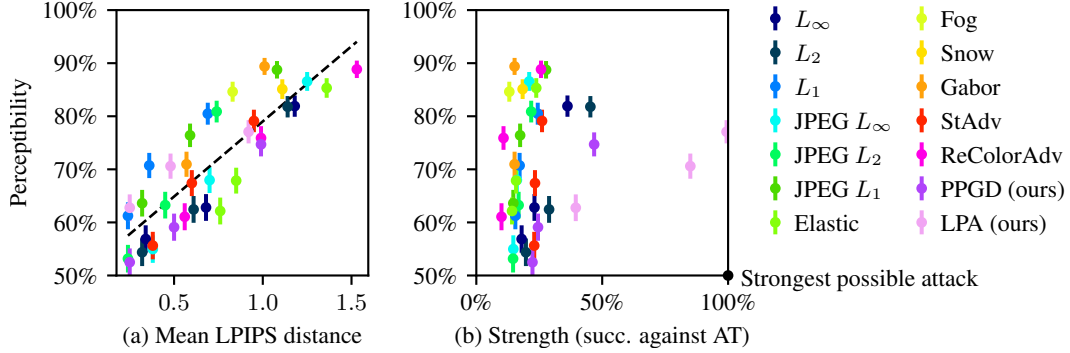


Figure 3: Results of the perceptual study described in Section 6 across twelve narrow threat models and our two perceptual attacks, each with three bounds. (a) The perceptibility of adversarial examples correlates well with the LPIPS distance (based on AlexNet) from the natural example. (b) The Lagrangian Perceptual Attack (LPA) is strongest at a given perceptibility, followed by L_2 , Perceptual PGD (PPGD), and L_∞ . Strength is the randomly targeted attack success rate against an adversarially trained classifier.

perceptual study. For each classifier, we determine the correlation between the mean LPIPS distance it assigns to image pairs from each attack and the perceptibility of that attack (Table 1). We find that AlexNet [35], trained normally on ImageNet [37], correlates best with human perception of these adversarial examples ($r = 0.84$); this agrees with Zhang et al. [22] who also find that AlexNet-based LPIPS correlates best with human perception (Figure 3). Because AlexNet is the best proxy for human judgements of perceptual distance, we use it for all externally-bounded evaluation attacks.

We also use the results of the perceptual study to investigate which attacks are strongest at a particular level of perceptibility. We evaluate each attack on a classifier hardened against that attack via adversarial training, and plot the resulting success rate against the proportion of correct annotations from the perceptual study. Out of the narrow threat models, we find that L_2 attacks are the strongest for their perceptibility. However, the Lagrangian Perceptual Attack (LPA) reduces a PAT-trained classifier to even lower accuracies (0.6% at the high bound), making it the strongest attack studied.

7 Experiments

We compare Perceptual Adversarial Training (PAT) to adversarial training against narrow threat models (L_p , spatial, etc.) on CIFAR-10 [38] and ImageNet-100 (the subset of ImageNet [37] containing every tenth class by WordNet ID order). We find that PAT results in classifiers with robustness against a broad range of narrow threat models. We also show that our perceptual attacks, PPGD and LPA, are strong against adversarial training with narrow threat models. We evaluate with externally-bounded PPGD and LPA (Section 4), using AlexNet to determine the LPIPS bound because it correlates best with human judgements (Table 1).

CIFAR-10 We test ResNet-50s trained on the CIFAR-10 dataset with PAT and adversarial training against six attacks (see Table 2): L_∞ and L_2 PGD [6], StAdv [10], ReColorAdv [12], and PPGD and LPA. This allows us to determine if PAT gives robustness against a range of adversarial attacks. We experiment with using various models to calculate the LPIPS distance during training. We try using the same model both for classification and to calculate the LPIPS distance (self-bounded PAT). We also use models pretrained normally or adversarially on CIFAR-10 prior to PAT (externally-bounded PAT) including AlexNet and ResNet-50. We find that PAT outperforms L_p adversarial training, particularly against the StAdv attack. Ablation studies of PAT are presented in Appendix E.

ImageNet-100 We compare the best-performing PAT variants, self-bounded and externally-bounded with AlexNet, to adversarial training against narrow threat models on ImageNet-100. Each resulting classifier is tested against twelve attacks at the large bound from the perceptual study (see Section 6 and Appendix Table 4). We use randomly-targeted attacks¹ to match Kang et al. [18].

¹Random targets are chosen for each input from all incorrect classes; an attack succeeds only if it perturbs the input such that the classifier outputs the target class. This is to maintain consistency with Kang et al. [18],

Table 2: Accuracies against various attacks for models trained with adversarial training and Perceptual Adversarial Training (PAT) variants on CIFAR-10. Attack bounds are 8/255 for L_∞ , 1 for L_2 , 0.5 for PPGD/LPA (bounded with AlexNet), and the original bounds for StAdv/ReColorAdv. All attacks are untargeted.

Training	LPIPS model	Attack						
		None	L_∞	L_2	StAdv	ReColorAdv	PPGD	LPA
Normal		95.2	0.0	0.0	0.0	0.6	0.2	0.0
AT L_∞		87.0	52.4	25.1	6.3	59.7	6.4	0.2
AT L_2		81.6	45.3	51.8	14.9	60.5	27.6	3.0
AT StAdv		83.9	0.3	0.8	76.1	13.9	0.1	0.0
AT ReColorAdv		92.0	15.5	10.5	0.3	81.2	1.8	0.0
PAT	self-bounded	81.9	42.3	47.2	51.7	75.4	26.5	5.8
PAT	AlexNet	85.9	41.5	46.5	15.4	64.0	31.8	3.3
PAT	ResNet-50	88.7	38.4	43.9	7.7	62.7	26.2	1.9
PAT	ResNet-50 (AT L_2)	75.8	52.0	58.1	68.3	73.2	32.9	8.7

Table 3: Comparison of adversarial training against narrow threat models and Perceptual Adversarial Training (PAT) on ImageNet-100. Accuracies are shown against twelve attacks with the large bounds from Table 4. All attacks are randomly targeted.¹ Gabor and Fog attacks are excluded because they have low success rates. Note that PAT gives high accuracy across diverse threat models.

Training	Attack												
	No	L_∞	L_2	L_1	J_∞	J_2	J_1	Snow	Elst	St	RC	PPGD	LPA
Normal	86.5	0.0	0.0	0.2	0.0	0.0	0.0	39.3	0.2	0.0	9.4	0.3	0.1
L_∞	78.5	63.9	9.0	32.9	18.5	8.6	2.9	76.6	33.0	5.2	40.4	18.7	0.3
L_2	75.0	60.5	54.4	72.9	68.2	64.4	36.2	73.6	42.4	16.7	37.3	40.6	0.4
L_1	83.5	1.1	0.4	75.7	5.2	5.7	2.9	75.3	6.1	1.0	19.5	0.8	0.1
JPEG- L_∞	83.9	2.2	0.1	19.4	79.0	75.4	47.0	72.1	2.7	0.4	28.9	0.7	0.0
JPEG- L_2	83.6	2.1	0.2	28.6	77.4	78.1	58.7	74.1	2.7	0.5	29.4	1.8	0.1
JPEG- L_1	82.6	5.3	0.9	45.3	78.1	79.4	71.9	76.2	6.4	0.9	32.3	1.8	0.1
Snow	83.2	0.0	0.0	0.6	0.0	0.0	0.0	81.4	1.9	0.1	10.7	0.1	0.0
Elastic	83.7	0.1	0.0	12.4	0.2	0.3	0.1	77.7	76.6	2.4	12.1	0.2	0.2
StAdv	77.1	2.7	1.1	55.1	8.2	5.7	13.6	76.0	75.2	73.7	13.2	2.0	0.2
ReColorAdv	90.0	0.1	0.0	0.6	0.0	0.0	0.0	83.4	1.1	0.1	74.3	0.1	0.2
PAT-self	72.8	59.5	51.4	70.7	63.6	58.6	40.9	71.5	50.5	43.2	51.6	55.7	2.0
PAT-AlexNet	78.1	63.1	51.8	75.4	68.6	62.1	39.1	76.9	47.1	23.9	47.7	53.3	0.6

The results are shown in Table 3. Both self- and externally-bounded PAT give similar results, and both produce robustness comparable to that of adversarial training across all attacks investigated. PAT is particularly impressive against the StAdv and ReColorAdv attacks, with accuracies over 10% higher than the next best model not trained against the specific attack.

Perceptual attacks On both CIFAR-10 and ImageNet-100, we find that Perceptual PGD (PPGD) and Lagrangian Perceptual Attack (LPA) are among the strongest attacks studied. LPA is the strongest, reducing the most robust classifier to 8.7% accuracy on CIFAR-10 and 2.0% accuracy on ImageNet-100. Furthermore, models most robust to LPA in both cases are those that have the best robustness across many narrow threat models. This demonstrates the utility of evaluating against LPA as a proxy for adversarial robustness against a range of threat models. See Appendix D for more experiments we have performed using variations of PPGD and LPA.

since we compare to their pretrained models. See Appendix F.1 for details.

8 Conclusion

We have presented attacks and defenses for the neural perceptual threat model (realized by the LPIPS distance) and shown that it closely approximates the true perceptual threat model, the set of all perturbations to natural inputs which fool a model but are imperceptible to humans. Our LPA attack is the strongest adversarial attack investigated, even in the presence of defenses. The proposed Perceptual Adversarial Training (PAT) improves robustness against a broad range of unseen attacks. While we have focused on image classifiers in this work, our approach is general and may be applied to other deep learning algorithms in which internal activations can be used to calculate similarity measures between inputs. Our proposed perceptual adversarial attacks and PAT could be extended to other vision algorithms, or even other domains such as audio and text.

Broader Impact

Perceptual adversarial training (PAT) could be used to robustify different computer vision systems, or even deep learning algorithms in other domains such as audio and text. Our perceptual attacks can be used to evaluate the adversarial robustness of trained computer vision algorithms against a wide threat model. However, we do not rule out that there may be stronger attacks within the true perceptual threat model. Thus, evaluation against our perceptual attacks may provide a false sense of security, and may need to be used as a necessary but not sufficient guarantor of robustness.

Adversarial robustness may be important for safety- or security-critical applications of deep learning, such as self-driving cars. Some work has shown successful adversarial attacks against object detectors [39] like those used in self-driving cars, which could fool the cars into taking unsafe actions. PAT may be used to improve the robustness of algorithms in these safety-critical applications, mitigating some of the risks. On the other hand, the attacks we describe, PPGD and LPA, are stronger than most existing attacks because they use a more expansive threat model. Thus, they could be used by attackers to fool security-critical machine learning systems into taking harmful actions.

This raises issues similar to those in the computer security research community; they debate the merits of full disclosure—making vulnerabilities public as soon as possible—versus responsible disclosure—giving time for the vulnerability to be patched before publication [40]. Responsible disclosure seems more difficult for adversarial attacks, since vulnerabilities may be widespread (not confined to a single piece of software) and vary greatly across applications.

Acknowledgments

This project was supported in part by NSF CAREER AWARD 1942230, HR 00111990077, HR001119S0026 and Simons Fellowship on “Foundations of Deep Learning.”

References

- [1] Battista Biggio, Igino Corona, Davide Maiorca, Blaine Nelson, Nedim Šrndić, Pavel Laskov, Giorgio Giacinto, and Fabio Roli. Evasion Attacks against Machine Learning at Test Time. In Hendrik Blockeel, Kristian Kersting, Siegfried Nijssen, and Filip Železný, editors, *Machine Learning and Knowledge Discovery in Databases*, Lecture Notes in Computer Science, pages 387–402, Berlin, Heidelberg, 2013. Springer. ISBN 978-3-642-40994-3. doi: 10.1007/978-3-642-40994-3_25.
- [2] Christian Szegedy, Wojciech Zaremba, Ilya Sutskever, Joan Bruna, Dumitru Erhan, Ian Goodfellow, and Rob Fergus. Intriguing properties of neural networks. In *International Conference on Learning Representations*, 2014. URL <http://arxiv.org/abs/1312.6199>.
- [3] Alexey Kurakin, Ian Goodfellow, and Samy Bengio. Adversarial examples in the physical world. *arXiv preprint arXiv:1607.02533*, 2016.
- [4] Cihang Xie, Jianyu Wang, Zhishuai Zhang, Yuyin Zhou, Lingxi Xie, and Alan Yuille. Adversarial examples for semantic segmentation and object detection. In *Proceedings of the IEEE International Conference on Computer Vision*, pages 1369–1378, 2017.
- [5] Ian Goodfellow, Jonathon Shlens, and Christian Szegedy. Explaining and Harnessing Adversarial Examples. In *International Conference on Learning Representations*, 2015.
- [6] Aleksander Madry, Aleksandar Makelov, Ludwig Schmidt, Dimitris Tsipras, and Adrian Vladu. Towards

- Deep Learning Models Resistant to Adversarial Attacks. In *International Conference on Learning Representations*, 2018.
- [7] Hongyang Zhang, Yaodong Yu, Jiantao Jiao, Eric P. Xing, Laurent El Ghaoui, and Michael I. Jordan. Theoretically Principled Trade-off Between Robustness and Accuracy. In *ICML*, 2019.
 - [8] Logan Engstrom, Brandon Tran, Dimitris Tsipras, Ludwig Schmidt, and Aleksander Madry. A Rotation and a Translation Suffice: Fooling CNNs with Simple Transformations. *arXiv preprint arXiv:1712.02779*, 2017.
 - [9] Eric Wong, Frank R. Schmidt, and J. Zico Kolter. Wasserstein Adversarial Examples via Projected Sinkhorn Iterations. *arXiv preprint arXiv:1902.07906*, February 2019. arXiv: 1902.07906.
 - [10] Chaowei Xiao, Jun-Yan Zhu, Bo Li, Warren He, Mingyan Liu, and Dawn Song. Spatially Transformed Adversarial Examples. *arXiv preprint arXiv:1801.02612*, 2018.
 - [11] Hossein Hosseini and Radha Poovendran. Semantic Adversarial Examples. In *Proceedings of the IEEE Conference on Computer Vision and Pattern Recognition Workshops*, pages 1614–1619, 2018.
 - [12] Cassidy Laidlaw and Soheil Feizi. Functional Adversarial Attacks. In *NeurIPS*, 2019.
 - [13] Anand Bhattad, Min Jin Chong, Kaizhao Liang, Bo Li, and David A. Forsyth. Big but Imperceptible Adversarial Perturbations via Semantic Manipulation. *arXiv preprint arXiv:1904.06347*, 2019.
 - [14] Yang Song, Rui Shu, Nate Kushman, and Stefano Ermon. Constructing Unrestricted Adversarial Examples with Generative Models. In *Proceedings of the 32nd International Conference on Neural Information Processing Systems*, pages 8322–8333. Curran Associates Inc., 2018.
 - [15] Xiaohui Zeng, Chenxi Liu, Yu-Siang Wang, Weichao Qiu, Lingxi Xie, Yu-Wing Tai, Chi Keung Tang, and Alan L. Yuille. Adversarial Attacks Beyond the Image Space. In *Proceedings of the IEEE Conference on Computer Vision and Pattern Recognition*, 2019. arXiv: 1711.07183.
 - [16] Matt Jordan, Naren Manoj, Surbhi Goel, and Alexandros G. Dimakis. Quantifying perceptual distortion of adversarial examples, 2019.
 - [17] Pratyush Maini, Eric Wong, and J. Zico Kolter. Adversarial Robustness Against the Union of Multiple Perturbation Models. *arXiv:1909.04068 [cs, stat]*, September 2019. URL <http://arxiv.org/abs/1909.04068>. arXiv: 1909.04068.
 - [18] Daniel Kang, Yi Sun, Dan Hendrycks, Tom Brown, and Jacob Steinhardt. Testing Robustness Against Unforeseen Adversaries. *arXiv preprint arXiv:1908.08016*, 2019.
 - [19] T. B. Brown, N. Carlini, C. Zhang, C. Olsson, P. Christiano, and I. Goodfellow. Unrestricted adversarial examples. *arXiv preprint arXiv:1809.08352*, 2018.
 - [20] Tom B. Brown, Dandelion Mané, Aurko Roy, Martín Abadi, and Justin Gilmer. Adversarial Patch. *arXiv:1712.09665 [cs]*, May 2018. URL <http://arxiv.org/abs/1712.09665>. arXiv: 1712.09665.
 - [21] Zhou Wang, A.C. Bovik, H.R. Sheikh, and E.P. Simoncelli. Image quality assessment: from error visibility to structural similarity. *IEEE Transactions on Image Processing*, 13(4):600–612, April 2004. ISSN 1941-0042. doi: 10.1109/TIP.2003.819861. Conference Name: IEEE Transactions on Image Processing.
 - [22] Richard Zhang, Phillip Isola, Alexei A. Efros, Eli Shechtman, and Oliver Wang. The Unreasonable Effectiveness of Deep Features as a Perceptual Metric. In *Proceedings of the IEEE Conference on Computer Vision and Pattern Recognition*, pages 586–595, 2018.
 - [23] Nicholas Carlini and David Wagner. Towards Evaluating the Robustness of Neural Networks. In *2017 IEEE Symposium on Security and Privacy (SP)*, pages 39–57. IEEE, 2017.
 - [24] Alexey Kurakin, Ian J. Goodfellow, and Samy Bengio. Adversarial machine learning at scale. *ArXiv*, abs/1611.01236, 2016.
 - [25] Aleksander Madry, Aleksandar Makelov, Ludwig Schmidt, Dimitris Tsipras, and Adrian Vladu. Towards deep learning models resistant to adversarial attacks. In *International Conference on Learning Representations*, 2018. URL <https://openreview.net/forum?id=rJzIBfZAb>.
 - [26] Hongyang Zhang, Yaodong Yu, Jiantao Jiao, Eric P. Xing, Laurent El Ghaoui, and Michael I. Jordan. Theoretically principled trade-off between robustness and accuracy. In *ICML*, 2019.
 - [27] Mahmood Sharif, Lujo Bauer, and Michael K. Reiter. On the Suitability of Lp-norms for Creating and Preventing Adversarial Examples. *arXiv:1802.09653 [cs]*, July 2018. URL <http://arxiv.org/abs/1802.09653>. arXiv: 1802.09653.
 - [28] Isaac Dunn, Tom Melham, and Daniel Kroening. Semantic Adversarial Perturbations using Learnt Representations. *arXiv:2001.11055 [cs]*, January 2020. URL <http://arxiv.org/abs/2001.11055>. arXiv: 2001.11055.
 - [29] Qiuling Xu, Guan hong Tao, Siyuan Cheng, Lin Tan, and Xiangyu Zhang. Towards Feature Space Adversarial Attack. *arXiv:2004.12385 [cs, eess]*, April 2020. URL <http://arxiv.org/abs/2004.12385>. arXiv: 2004.12385.

- [30] Z. Wang, E.P. Simoncelli, and A.C. Bovik. Multiscale structural similarity for image quality assessment. In *The Thirty-Seventh Asilomar Conference on Signals, Systems Computers, 2003*, volume 2, pages 1398–1402 Vol.2, November 2003. doi: 10.1109/ACSSC.2003.1292216.
- [31] Mehul P. Sampat, Zhou Wang, Shalini Gupta, Alan Conrad Bovik, and Mia K. Markey. Complex Wavelet Structural Similarity: A New Image Similarity Index. *IEEE Transactions on Image Processing*, 18(11): 2385–2401, November 2009. ISSN 1941-0042. doi: 10.1109/TIP.2009.2025923. Conference Name: IEEE Transactions on Image Processing.
- [32] Rafał Mantiuk, Kil Joong Kim, Allan G. Rempel, and Wolfgang Heidrich. HDR-VDP-2: a calibrated visual metric for visibility and quality predictions in all luminance conditions. *ACM Transactions on Graphics*, 30(4):40:1–40:14, July 2011. ISSN 0730-0301. doi: 10.1145/2010324.1964935. URL <https://doi.org/10.1145/2010324.1964935>.
- [33] Yogesh Balaji, Tom Goldstein, and Judy Hoffman. Instance adaptive adversarial training: Improved accuracy tradeoffs in neural nets. *arXiv:1910.08051 [cs, stat]*, October 2019. URL <http://arxiv.org/abs/1910.08051>. arXiv: 1910.08051.
- [34] Kaiming He, Xiangyu Zhang, Shaoqing Ren, and Jian Sun. Deep Residual Learning for Image Recognition. In *Proceedings of the IEEE Conference on Computer Vision and Pattern Recognition*, pages 770–778, 2016.
- [35] Alex Krizhevsky, Ilya Sutskever, and Geoffrey E Hinton. ImageNet Classification with Deep Convolutional Neural Networks. In F. Pereira, C. J. C. Burges, L. Bottou, and K. Q. Weinberger, editors, *Advances in Neural Information Processing Systems 25*, pages 1097–1105. Curran Associates, Inc., 2012. URL <http://papers.nips.cc/paper/4824-imagenet-classification-with-deep-convolutional-neural-networks.pdf>.
- [36] Karen Simonyan and Andrew Zisserman. Very Deep Convolutional Networks for Large-Scale Image Recognition. September 2014. URL <https://arxiv.org/abs/1409.1556v6>.
- [37] Olga Russakovsky, Jia Deng, Hao Su, Jonathan Krause, Sanjeev Satheesh, Sean Ma, Zhiheng Huang, Andrej Karpathy, Aditya Khosla, Michael Bernstein, Alexander C. Berg, and Li Fei-Fei. ImageNet Large Scale Visual Recognition Challenge. *International Journal of Computer Vision (IJCV)*, 115(3):211–252, 2015. doi: 10.1007/s11263-015-0816-y.
- [38] Alex Krizhevsky and Geoffrey Hinton. Learning Multiple Layers of Features from Tiny Images. Technical report, Citeseer, 2009.
- [39] Kevin Eykholt, Ivan Evtimov, Earlene Fernandes, Bo Li, Amir Rahmati, Chaowei Xiao, Atul Prakash, Tadayoshi Kohno, and Dawn Song. Robust Physical-World Attacks on Deep Learning Models. In *CVPR 2018*, April 2018. arXiv: 1707.08945.
- [40] Stefan Frei, Dominik Schatzmann, Bernhard Plattner, and Brian Trammell. Modeling the Security Ecosystem - The Dynamics of (In)Security. In Tyler Moore, David Pym, and Christos Ioannidis, editors, *Economics of Information Security and Privacy*, pages 79–106, Boston, MA, 2010. Springer US. ISBN 978-1-4419-6967-5. doi: 10.1007/978-1-4419-6967-5_6.
- [41] Hossein Hosseini, Baicen Xiao, Mayoore Jaiswal, and Radha Poovendran. On the Limitation of Convolutional Neural Networks in Recognizing Negative Images. In *16th IEEE International Conference on Machine Learning and Applications (ICMLA)*, pages 352–358. IEEE, 2017.
- [42] Huan Zhang, Hongge Chen, Zhao Song, Duane S. Boning, Inderjit S. Dhillon, and Cho-Jui Hsieh. The Limitations of Adversarial Training and the Blind-Spot Attack. *International Conference on Learning Representations*, 2019.
- [43] Adam Paszke, Sam Gross, Soumith Chintala, Gregory Chanan, Edward Yang, Zachary DeVito, Zeming Lin, Alban Desmaison, Luca Antiga, and Adam Lerer. Automatic Differentiation in PyTorch. In *NIPS-W*, 2017.
- [44] Logan Engstrom, Andrew Ilyas, Shibani Santurkar, and Dimitris Tsipras. Robustness (python library), 2019. URL <https://github.com/MadryLab/robustness>.

Appendix

A Perceptual Attack Algorithms

A.1 Perceptual PGD

Recall from Section 4 that Perceptual PGD (PPGD) consists of repeatedly applying two steps: a first-order step in LPIPS distance to maximize the loss, followed by a projection into the allowed set of inputs. Here, we focus on the first-order step; see Appendix A.4 for how we perform projection onto the LPIPS ball.

We wish to solve the following constrained optimization for the step δ given the step size η and current input \mathbf{x} :

$$\max_{\delta} \mathcal{L}(f(\mathbf{x} + \delta), y) \quad \text{subject to} \quad \|J\delta\|_2 \leq \eta \quad (7)$$

Let $\hat{f}(\mathbf{x}) := \mathcal{L}(f(\mathbf{x}), y)$ for an input $\mathbf{x} \in \mathcal{X}$. Let J be the Jacobian of $\phi(\cdot)$ at \mathbf{x} and $\nabla \hat{f}$ be the gradient of $\hat{f}(\cdot)$ at \mathbf{x} .

Lemma 1. *The first-order approximation of (7) is*

$$\max_{\delta} \hat{f}(\mathbf{x}) + (\nabla \hat{f})^\top \delta \quad \text{subject to} \quad \|J\delta\|_2 \leq \eta, \quad (8)$$

and can be solved in closed-form by

$$\delta^* = \eta \frac{(J^\top J)^{-1}(\nabla \hat{f})}{\|(J^+)^{\top}(\nabla \hat{f})\|_2}.$$

where J^+ is the pseudoinverse of J .

Proof. We solve (8) using Lagrange multipliers. First, we take the gradient of the objective:

$$\nabla_{\delta} [\hat{f}(\mathbf{x}) + (\nabla \hat{f})^\top \delta] = \nabla \hat{f}$$

We can rewrite the constraint by squaring both sides to obtain

$$\delta^\top J^\top J \delta - \eta^2 \leq 0$$

Taking the gradient of the constraint gives

$$\nabla_{\delta} [\delta^\top J^\top J \delta - \eta^2] = 2J^\top J \delta$$

Now, we set one gradient as a multiple of the other and solve for δ :

$$J^\top J \delta = \lambda(\nabla \hat{f}) \quad (9)$$

$$\delta = \lambda(J^\top J)^{-1}(\nabla \hat{f}) \quad (10)$$

Substituting into the constraint from (8) gives

$$\begin{aligned} \|J\delta\|_2 &= \eta \\ \|J\lambda(J^\top J)^{-1}(\nabla \hat{f})\|_2 &= \eta \\ \lambda\|J(J^\top J)^{-1}(\nabla \hat{f})\|_2 &= \eta \\ \lambda\|((J^\top J)^{-1}J^\top)^\top(\nabla \hat{f})\|_2 &= \eta \\ \lambda\|(J^+)^{\top}(\nabla \hat{f})\|_2 &= \eta \\ \lambda &= \frac{\eta}{\|(J^+)^{\top}(\nabla \hat{f})\|_2} \end{aligned}$$

We substitute this value of λ into (10) to obtain

$$\delta^* = \eta \frac{(J^\top J)^{-1}(\nabla \hat{f})}{\|(J^+)^{\top}(\nabla \hat{f})\|_2}. \quad (11)$$

■

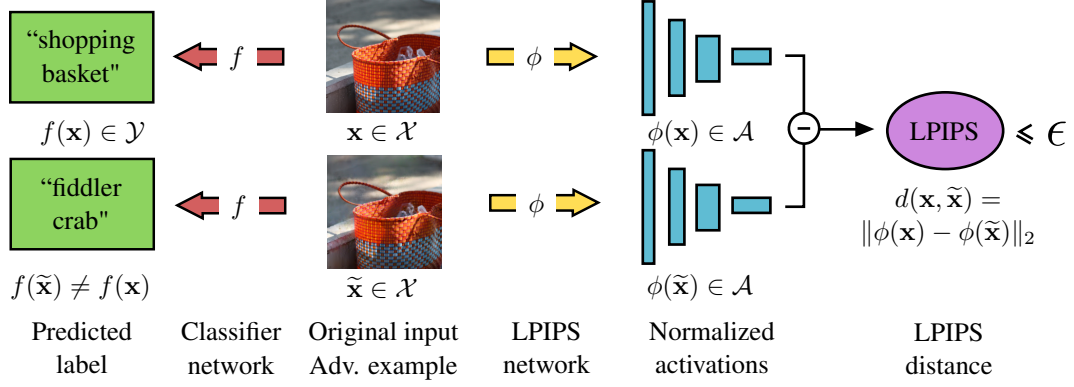


Figure 4: Creating an adversarial example in the LPIPS threat model.

Solution with conjugate gradient method Calculating (11) directly is computationally intractable for most neural networks, since inverting $J^\top J$ and calculating the pseudoinverse of J are expensive. Instead, we approximate δ^* by using the conjugate gradient method to solve the following linear system, based on (9):

$$J^\top J \delta = \nabla \hat{f} \quad (12)$$

$\nabla \hat{f}$ is easy to calculate using backpropagation. The conjugate gradient method does not require calculating fully $J^\top J$; instead, it only requires the ability to perform matrix-vector products $J^\top J v$ for various vectors v .

We can approximate $J v$ using finite differences given a small, positive value h :

$$J v \approx \frac{\phi(\mathbf{x} + h v) - \phi(\mathbf{x})}{h}$$

Then, we can calculate $J^\top J v$ by introducing an additional variable u and using autograd:

$$\begin{aligned} \nabla_u \left[(\phi(x + u))^\top J v \right]_{u=0} &= \left[\left(\frac{d\phi}{du}(x + u) \right)^\top J v + (\phi(x + u))^\top \frac{d}{du} J v \right]_{u=0} \\ &= \left[\left(\frac{d\phi}{du}(x + u) \right)^\top J v + (\phi(x + u))^\top \mathbf{0} \right]_{u=0} \\ &= \left(\frac{d\phi}{du}(x) \right)^\top J v = J^\top J v \end{aligned}$$

This allows us to efficiently approximate the solution of (12) to obtain $(J^\top J)^{-1} \nabla \hat{f}$. We use 5 iterations of the conjugate gradient algorithm in practice.

From there, it is easy to solve for λ , given that $(J^+)^{\top} \nabla \hat{f} = J(J^\top J)^{-1} \nabla \hat{f}$. Then, δ^* can be calculated via (10). See Algorithm 1 for the full attack.

Computational complexity PPGD's running time scales with the number of steps T and the number of conjugate gradient iterations K . It also depends on whether the attack is self-bounded (the same network is used for classification and the LPIPS distance) or externally-bounded (different networks are used).

For each of the T steps, $\theta(\tilde{\mathbf{x}})$, $\nabla_{\tilde{\mathbf{x}}} \mathcal{L}(f(\tilde{\mathbf{x}}), y)$, and $\phi(\tilde{\mathbf{x}} + h \delta_k)$ must be calculated once (lines 4 and 15 in Algorithm 1). This takes 2 forward passes and 1 backward pass for the self-bounded case, and 3 forward passes and 1 backward pass for the externally-bounded case.

In addition, $J^\top J v$ needs to be calculated (in the MULTIPLYJACOBIAN routine) $K + 1$ times. Each calculation of $J^\top J v$ requires 1 forward and 1 backward pass, assuming $\phi(\tilde{\mathbf{x}})$ is already calculated.

Finally, the projection step takes $n + 1$ forward passes for n iterations of the bisection method (see Section A.4).

In all, the algorithm requires $T(K + n + 4)$ forward passes and $T(K + n + 3)$ backward passes in the self-bounded case. In the externally-bounded case, it requires $T(K + n + 5)$ forward passes and the same number of backward passes.

Algorithm 1 Perceptual PGD (PPGD)

```

1: procedure PPGD(classifier  $f(\cdot)$ , LPIPS network  $\phi(\cdot)$ , input  $\mathbf{x}$ , label  $y$ , bound  $\epsilon$ , step  $\eta$ )
2:    $\tilde{\mathbf{x}} \leftarrow \mathbf{x} + 0.01 * \mathcal{N}(0, 1)$   $\triangleright$  initialize perturbations with random Gaussian noise
3:   for  $t$  in  $1, \dots, T$  do  $\triangleright T$  is the number of steps
4:      $\nabla \hat{f} \leftarrow \nabla_{\tilde{\mathbf{x}}} \mathcal{L}(f(\tilde{\mathbf{x}}), y)$ 
5:      $\delta_0 \leftarrow 0$ 
6:      $r_0 \leftarrow \nabla \hat{f} - \text{MULTIPLYJACOBIAN}(\phi, \tilde{\mathbf{x}}, \delta_0)$ 
7:      $p_0 \leftarrow r_0$ 
8:     for  $k$  in  $0, \dots, K - 1$  do  $\triangleright$  conjugate gradient algorithm; we use  $K = 5$  iterations
9:        $\alpha_k \leftarrow \frac{r_k^\top r_k}{p_k^\top \text{MULTIPLYJACOBIAN}(\phi, \tilde{\mathbf{x}}, p_k)}$ 
10:       $\delta_{k+1} \leftarrow \delta_k + \alpha_k p_k$ 
11:       $r_{k+1} \leftarrow r_k - \alpha_k \text{MULTIPLYJACOBIAN}(\phi, \tilde{\mathbf{x}}, p_k)$ 
12:       $\beta_k \leftarrow \frac{r_{k+1}^\top r_{k+1}}{r_k^\top r_k}$ 
13:       $p_{k+1} \leftarrow r_{k+1} + \beta_k p_k$ 
14:    end for
15:     $m \leftarrow \|\phi(\tilde{\mathbf{x}} + h\delta_k) - \phi(\tilde{\mathbf{x}})\|/h$   $\triangleright m \approx \|J\delta_k\|$  for small  $h$ ; we use  $h = 10^{-3}$ 
16:     $\tilde{\mathbf{x}} \leftarrow (\eta/m)\delta_k$ 
17:     $\tilde{\mathbf{x}} \leftarrow \text{PROJECT}(d, \tilde{\mathbf{x}}, \mathbf{x}, \epsilon)$ 
18:  end for
19:  return  $\tilde{\mathbf{x}}$ 
20: end procedure
21:
22: procedure MULTIPLYJACOBIAN( $\phi(\cdot)$ ,  $\tilde{\mathbf{x}}$ ,  $\mathbf{v}$ )  $\triangleright$  calculates  $J^\top J\mathbf{v}$ ;  $J$  is the Jacobian of  $\phi$  at  $\tilde{\mathbf{x}}$ 
23:    $J\mathbf{v} \leftarrow (\phi(\tilde{\mathbf{x}} + h\mathbf{v}) - \phi(\tilde{\mathbf{x}}))/h$   $\triangleright h$  is a small positive value; we use  $h = 10^{-3}$ 
24:    $J^\top J\mathbf{v} \leftarrow \nabla_{\mathbf{u}} [\phi(\tilde{\mathbf{x}} + \mathbf{u})^\top J\mathbf{v}]_{\mathbf{u}=0}$ 
25:   return  $J^\top J\mathbf{v}$ 
26: end procedure

```

A.2 Lagrangian Perceptual Attack (LPA)

Our second attack, Lagrangian Perceptual Attack (LPA), optimizes a Lagrangian relaxation of the perceptual attack problem (3):

$$\max_{\tilde{\mathbf{x}}} \quad \mathcal{L}(f(\tilde{\mathbf{x}}), y) - \lambda \max \left(0, \|\phi(\tilde{\mathbf{x}}) - \phi(\mathbf{x})\|_2 - \epsilon \right). \quad (13)$$

To optimize (13), we use a variation of gradient descent over $\tilde{\mathbf{x}}$, starting at \mathbf{x} with a small amount of noise added. We perform our modified version of gradient descent for T steps. We use a step size η , which begins at ϵ and decays exponentially to $\epsilon/10$.

At each step, we begin by taking the gradient of (13) with respect to $\tilde{\mathbf{x}}$; let Δ refer to this gradient. Then, we normalize Δ to have L_2 norm 1, i.e. $\hat{\Delta} = \Delta/\|\Delta\|_2$. We wish to take a step in the direction of $\hat{\Delta}$ of size η in LPIPS distance. If we wanted to take a step of size η in L_2 distance, we could just take the step $\eta\hat{\Delta}$. However, taking a step of particular size in LPIPS distance is harder. We assume that the LPIPS distance is approximately linear in the direction $\hat{\Delta}$. We can approximate the directional derivative of the LPIPS distance in the direction $\hat{\Delta}$ using finite differences:

$$\frac{d}{d\alpha} d(\tilde{\mathbf{x}}, \tilde{\mathbf{x}} + \alpha\hat{\Delta}) \approx \frac{d(\tilde{\mathbf{x}}, \tilde{\mathbf{x}} + h\hat{\Delta})}{h} = m.$$

Here, h is a small positive value, and we assign the approximation of the directional derivative to m .

Now, we can write the first-order Taylor expansion of the perceptual distance towards the direction $\hat{\Delta}$ as follows:

$$d(\tilde{\mathbf{x}}, \tilde{\mathbf{x}} + \alpha \hat{\Delta}) \approx d(\tilde{\mathbf{x}}, \tilde{\mathbf{x}}) + m\alpha = m\alpha.$$

we want to take a step of size η . Plugging in and solving, we obtain

$$\begin{aligned}\eta &= d(\tilde{\mathbf{x}}, \tilde{\mathbf{x}} + \alpha \hat{\Delta}) \approx m\alpha \\ \eta &\approx m\alpha \\ \eta/m &\approx \alpha.\end{aligned}$$

So, the approximate step we should take is $(\eta/m)\hat{\Delta}$. We take this step at each of the T iterations of our modified gradient descent method.

We begin with $\lambda = 10^{-2}$. After performing gradient descent, if $d(\mathbf{x}, \tilde{\mathbf{x}}) > \epsilon$ (i.e. the adversarial example is outside the constraint) we increase λ by a factor of 10 and repeat the optimization. We repeat this entire process five times, meaning we search over $\lambda \in \{10^{-2}, 10^{-1}, 10^0, 10^1, 10^2\}$. Finally, if the resulting adversarial example is still outside the constraint, we project it into the threat model; see Appendix 4.

Computational complexity LPA’s running time scales with the number of iterations S used to search for λ as well as the number of gradient descent steps T . $\phi(\mathbf{x})$ may be calculated once during the entire attack, which speeds it up. Then, each step of gradient descent requires 2 forward and 1 backward passes in the self-bounded case, and 3 forward and 2 backward passes in the externally-bounded case.

The projection at the end of the attack requires $n + 1$ forward passes for n iterations of the bisection method (see Section A.4).

In total, the attack requires $2ST + n + 2$ forward passes and $ST + n + 2$ backward passes in the self-bounded case, and $3ST + n + 2$ forward passes and $2ST + n + 2$ backward passes in the externally-bounded case.

Algorithm 2 Lagrangian Perceptual Attack (LPA)

```

1: procedure LPA(classifier network  $f(\cdot)$ , LPIPS distance  $d(\cdot, \cdot)$ , input  $\mathbf{x}$ , label  $y$ , bound  $\epsilon$ )
2:    $\lambda \leftarrow 0.01$ 
3:    $\tilde{\mathbf{x}} \leftarrow \mathbf{x} + 0.01 * \mathcal{N}(0, 1)$  ▷ initialize perturbations with random Gaussian noise
4:   for  $i$  in  $1, \dots, S$  do ▷ we use  $S = 5$  iterations to search for the best value of  $\lambda$ 
5:     for  $t$  in  $1, \dots, T$  do ▷  $T$  is the number of steps
6:        $\Delta \leftarrow \nabla_{\tilde{\mathbf{x}}} [\mathcal{L}(f(\tilde{\mathbf{x}}), y) - \lambda \max(0, d(\tilde{\mathbf{x}}, \mathbf{x}) - \epsilon)]$  ▷ take the gradient of (5)
7:        $\hat{\Delta} = \Delta / \|\Delta\|_2$  ▷ normalize the gradient
8:        $\eta = \epsilon * (0.1)^{t/T}$  ▷ the step size  $\eta$  decays exponentially
9:        $m \leftarrow d(\tilde{\mathbf{x}}, \tilde{\mathbf{x}} + h\hat{\Delta})/h$  ▷  $m \approx$  derivative of  $d(\tilde{\mathbf{x}}, \cdot)$  in the direction of  $\hat{\Delta}$ ;  $h = 0.1$ 
10:       $\tilde{\mathbf{x}} \leftarrow \tilde{\mathbf{x}} + (\eta/m)\hat{\Delta}$  ▷ take a step of size  $\eta$  in LPIPS distance
11:    end for
12:    if  $d(\tilde{\mathbf{x}}, \mathbf{x}) > \epsilon$  then
13:       $\lambda \leftarrow 10\lambda$  ▷ increase  $\lambda$  if the attack goes outside the bound
14:    end if
15:  end for
16:   $\tilde{\mathbf{x}} \leftarrow \text{PROJECT}(d, \tilde{\mathbf{x}}, \mathbf{x}, \epsilon)$ 
17:  return  $\tilde{\mathbf{x}}$ 
18: end procedure
```

A.3 Fast Lagrangian Perceptual Attack

We use the Fast Lagrangian Perceptual Attack (Fast-LPA) for Perceptual Adversarial Training (PAT, see Section 5). Fast-LPA is similar to LPA (Appendix A.2), with two major differences. First, Fast-LPA does not search over λ values; instead, during the T gradient descent steps, λ is increased exponentially from 1 to 10. Second, we remove the projection step at the end of the attack. This means that Fast-LPA may produce adversarial examples outside the threat model. This means that

Fast-LPA cannot be used for evaluation, but it is fine for training.

Computational complexity Fast-LPA’s running time can be calculated similarly to LPA’s (see Section A.2), except that $S = 1$ and there is no projection step. Let T be the number of steps taken during the attack. Then Fast-LPA requires $2T + 1$ forward passes and $T + 1$ backward passes for the self-bounded case, and $3T + 1$ forward passes and $2T + 1$ backward passes for the externally-bounded case.

In comparison, PGD with T iterations requires T forward passes and T backward passes. Thus, Fast-LPA is slightly slower, requiring $T + 1$ more forward passes and no more backward passes.

Algorithm 3 Fast Lagrangian Perceptual Attack (Fast-LPA)

```

1: procedure FASTLPA(classifier network  $f(\cdot)$ , LPIPS distance  $d(\cdot, \cdot)$ , input  $\mathbf{x}$ , label  $y$ , bound  $\epsilon$ )
2:    $\tilde{\mathbf{x}} \leftarrow \mathbf{x} + 0.01 * \mathcal{N}(0, 1)$   $\triangleright$  initialize perturbations with random Gaussian noise
3:   for  $t$  in  $1, \dots, T$  do  $\triangleright T$  is the number of steps
4:      $\lambda \leftarrow 10^{t/T}$   $\triangleright \lambda$  increases exponentially
5:      $\Delta \leftarrow \nabla_{\tilde{\mathbf{x}}} [\mathcal{L}(f(\tilde{\mathbf{x}}), y) - \lambda \max(0, d(\tilde{\mathbf{x}}, \mathbf{x}) - \epsilon)]$   $\triangleright$  take the gradient of (5)
6:      $\hat{\Delta} = \Delta / \|\Delta\|_2$   $\triangleright$  normalize the gradient
7:      $\eta = \epsilon * (0.1)^{t/T}$   $\triangleright$  the step size  $\eta$  decays exponentially
8:      $m \leftarrow d(\tilde{\mathbf{x}}, \tilde{\mathbf{x}} + h\hat{\Delta})/h$   $\triangleright m \approx$  derivative of  $d(\tilde{\mathbf{x}}, \cdot)$  in the direction of  $\hat{\Delta}$ ;  $h = 0.1$ 
9:      $\tilde{\mathbf{x}} \leftarrow \tilde{\mathbf{x}} + (\eta/m)\hat{\Delta}$   $\triangleright$  take a step of size  $\eta$  in LPIPS distance
10:  end for
11:  return  $\tilde{\mathbf{x}}$ 
12: end procedure

```

A.4 Perceptual Projection

We explored two methods of projecting adversarial examples into the LPIPS threat model. The method we use throughout the paper is based on the bisection root finding method and is shown in Algorithm 4. However, we also explored using Newton’s method, shown in Algorithm 5 (also see Appendix D).

In general, given an adversarial example $\tilde{\mathbf{x}}$, original input \mathbf{x} , and LPIPS bound ϵ , we wish to find a projection $\tilde{\mathbf{x}}'$ of $\tilde{\mathbf{x}}$ such that $d(\tilde{\mathbf{x}}', \mathbf{x}) \leq \epsilon$. Assume for this section that $d(\tilde{\mathbf{x}}, \mathbf{x}) > \epsilon$, i.e. the current adversarial example $\tilde{\mathbf{x}}$ is outside the bound. If $d(\tilde{\mathbf{x}}, \mathbf{x}) \leq \epsilon$, then we can just let $\tilde{\mathbf{x}}' = \tilde{\mathbf{x}}$ and be done.

Bisection method The first projection method we explored (and the one we use throughout the paper) attempts to find a projection $\tilde{\mathbf{x}}'$ along the line connecting the current adversarial example $\tilde{\mathbf{x}}$ and original input \mathbf{x} . Let $\delta = \tilde{\mathbf{x}} - \mathbf{x}$. Then we can represent our final projection $\tilde{\mathbf{x}}'$ as a point between \mathbf{x} and $\tilde{\mathbf{x}}$ as

$$\tilde{\mathbf{x}}' = \mathbf{x} + \alpha\delta,$$

for some $\alpha \in [0, 1]$. If $\alpha = 0$, $\tilde{\mathbf{x}}' = \mathbf{x}$; if $\alpha = 1$, $\tilde{\mathbf{x}}' = \tilde{\mathbf{x}}$. Now, define a function $r : [0, 1] \rightarrow \mathbb{R}$ as

$$r(\delta) = d(\mathbf{x} + \alpha\delta, \mathbf{x}) - \epsilon.$$

This function has the following properties:

1. $r(0) < 0$, since $r(0) = d(\mathbf{x}, \mathbf{x}) - \epsilon = -\epsilon$.
2. $r(1) > 0$, since $r(1) = d(\tilde{\mathbf{x}}, \mathbf{x}) - \epsilon > 0$ because $d(\tilde{\mathbf{x}}, \mathbf{x}) > \epsilon$.
3. $r(\alpha) = 0$ iff $d(\tilde{\mathbf{x}}', \mathbf{x}) = \epsilon$.

We use the bisection root finding method to find a root α^* of $r(\cdot)$ on the interval $[0, 1]$, which exists since $r(\cdot)$ is continuous and because of items 1 and 2 above. By item 3, at this root, the projected adversarial example is within the threat model:

$$d(\tilde{\mathbf{x}}', \mathbf{x}) = d(\mathbf{x} + \alpha^*\delta, \mathbf{x}) = r(\alpha^*) + \epsilon = \epsilon$$

We use $n = 10$ iterations of the bisection method to calculate α^* . This requires $n + 1$ forward passes through the LPIPS network, since $\phi(\mathbf{x})$ must be calculated once, and $\phi(\mathbf{x} + \alpha\delta)$ must be calculated

n times. See Algorithm 4 for the full projection algorithm.

Algorithm 4 Perceptual Projection (Bisection Method)

```

procedure PROJECT(LPIPS distance  $d(\cdot, \cdot)$ , adversarial example  $\tilde{\mathbf{x}}$ , original input  $\mathbf{x}$ , bound  $\epsilon$ )
   $\alpha_{\min}, \alpha_{\max} \leftarrow 0, 1$ 
   $\delta \leftarrow \tilde{\mathbf{x}} - \mathbf{x}$ 
  for  $i$  in  $1, \dots, n$  do
     $\alpha \leftarrow (\alpha_{\min} + \alpha_{\max})/2$ 
     $\tilde{\mathbf{x}}' \leftarrow \mathbf{x} + \alpha\delta$ 
    if  $d(\mathbf{x}, \tilde{\mathbf{x}}') > \epsilon$  then
       $\alpha_{\max} \leftarrow \alpha$ 
    else
       $\alpha_{\min} \leftarrow \alpha$ 
    end if
  end for
  return  $\tilde{\mathbf{x}}'$ 
end procedure

```

Newton’s method The second projection method we explored uses the generalized Newton–Raphson method to attempt to find the closest projection $\tilde{\mathbf{x}}'$ to the current adversarial example $\tilde{\mathbf{x}}$ such that the projection is within the threat model, i.e. $d(\tilde{\mathbf{x}}', \mathbf{x}) \leq \epsilon$. To find such a projection, we again define a function $r(\cdot)$ and look for its roots:

$$r(\tilde{\mathbf{x}}') = d(\tilde{\mathbf{x}}', \mathbf{x}) - \epsilon.$$

If we can find a projection $\tilde{\mathbf{x}}'$ close to $\tilde{\mathbf{x}}$ such that $r(\tilde{\mathbf{x}}') \leq 0$, then this projection will be contained within the threat model, since

$$r(\tilde{\mathbf{x}}') \leq 0 \Rightarrow d(\tilde{\mathbf{x}}', \mathbf{x}) \leq \epsilon.$$

To find such a root, we use the generalized Newton-Raphson method, an iterative algorithm. Beginning with $\tilde{\mathbf{x}}'_0 = \tilde{\mathbf{x}}$, we update $\tilde{\mathbf{x}}'$ iteratively using the step

$$\tilde{\mathbf{x}}'_{i+1} = \tilde{\mathbf{x}}'_i - \left[\nabla r(\tilde{\mathbf{x}}'_i) \right]^+ \left(r(\tilde{\mathbf{x}}'_i) + s \right),$$

where A^+ denotes the pseudoinverse of A , and s is a small positive constant (the “overshoot”), which helps the algorithm converge. We continue this process until $r(\tilde{\mathbf{x}}'_t) \leq 0$, at which point the projection is complete.

This algorithm usually takes 2-3 steps to converge with $s = 10^{-2}$. Each step requires 1 forward and 1 backward pass to calculate $r(\tilde{\mathbf{x}}'_t)$ and its gradient. The method also requires 1 forward pass at the beginning to calculate $\phi(\mathbf{x})$.

Algorithm 5 Perceptual Projection (Newton’s Method)

```

procedure PROJECT(LPIPS distance  $d(\cdot, \cdot)$ , adversarial example  $\tilde{\mathbf{x}}$ , original input  $\mathbf{x}$ , bound  $\epsilon$ )
   $\tilde{\mathbf{x}}'_0 \leftarrow \tilde{\mathbf{x}}$ 
  for  $i$  in  $0, \dots$  do
     $r(\tilde{\mathbf{x}}'_i) \leftarrow d(\tilde{\mathbf{x}}'_i, \mathbf{x}) - \epsilon$ 
    if  $r(\tilde{\mathbf{x}}'_i) \leq 0$  then
      return  $\tilde{\mathbf{x}}'_i$ 
    end if
     $\tilde{\mathbf{x}}'_{i+1} = \tilde{\mathbf{x}}'_i - \left[ \nabla r(\tilde{\mathbf{x}}'_i) \right]^+ \left( r(\tilde{\mathbf{x}}'_i) + s \right)$ 
  end for
end procedure

```

$\triangleright s$ is the “overshoot”; we use $s = 10^{-2}$

B Additional Related Work

Here, we expand on the related work discussed in Section 2 discuss some additional existing work on adversarial robustness.

Adversarial attacks Much of the initial work on adversarial robustness focused on perturbations to natural images which were bounded by the L_2 or L_∞ distance [23, 5, 6]. However, recently the community has discovered many other types of perturbations that are imperceptible and can be optimized to fool a classifier, but are outside L_p threat models. These include spatial perturbations using flow fields [10], translation and rotation [8], and Wasserstein distance bounds [9]. Attacks that manipulate the colors in images uniformly also been proposed [11, 41, 42] and have been generalized into “functional adversarial attacks” by Laidlaw and Feizi [12].

A couple papers have proposed adversarial threat models that do not focus on a simple, manually defined perturbation type. Dunn et al. [28] use a generative model of images; they perturb the features at various layers in the generator to create adversarial examples. Xu et al. [29] train an autoencoder and then perturb images in representation space rather than pixel space.

C Additional Perceptual Study Results

Table 4: Bounds and results from the perceptual study. Each threat model was evaluated with a small, medium, and large bound. Bounds for UAR attacks (first ten rows) are given assuming input image is in the range $[0, 255]$. Perceptibility (perc.) is the proportion of natural input-adversarial example pairs annotated correctly by participants. Strength (str.) is the success rate when attacking a classifier adversarially trained against that threat model (higher is stronger). Perceptual attacks (PPGD and LPA, see Section 4) are externally bounded with AlexNet. A dash (—) indicates that none of the UAR attack bounds from Kang et al. [18] were imperceptible enough. All experiments on ImageNet-100.

Threat model	Small bound			Medium bound			Large bound		
	Bound	Perc.	Str.	Bound	Perc.	Str.	Bound	Perc.	Str.
L_∞	2	57%	18.0%	4	63%	23.1%	8	82%	36.2%
L_2	600	54%	19.7%	1200	62%	28.9%	2400	82%	45.3%
L_1	9562.5	61%	15.5%	19125	71%	17.2%	76500	80%	24.4%
JPEG- L_∞	0.0625	55%	14.7%	0.125	68%	16.1%	0.25	87%	21.0%
JPEG- L_2	8	53%	14.6%	16	63%	16.8%	32	81%	21.8%
JPEG- L_1	256	64%	14.7%	1024	76%	17.4%	4096	89%	27.7%
Fog		—			—		128	85%	13.1%
Gabor		—		6.25	71%	15.2%	12.5	89%	15.2%
Snow		—			—		0.0625	85%	18.4%
Elastic	0.25	62%	14.2%	0.5	68%	15.8%	2	85%	23.8%
StAdv	0.025	56%	23.0%	0.05	67%	23.3%	0.1	79%	26.1%
ReColorAdv	0.03	61%	10.0%	0.06	76%	10.8%	0.12	89%	25.7%
PPGD	0.25	53%	22.3%	0.5	59%	24.5%	1	75%	46.8%
LPA	0.25	63%	39.5%	0.5	71%	85.0%	1	77%	99.4%

D Perceptual Attack Experiments

We experiment with variations of the two validation attacks, PPGD and LPA, described in Section 4. As described in Appendix A.4, we developed two methods for projecting candidate adversarial examples into the LPIPS ball surrounding a natural input. We attack a single model using PPGD and LPA with both projection methods. We also compare self-bounded to externally-bounded attacks.

We find that LPA tends to be more powerful than PPGD. Finally, we note that externally-bounded LPA is extremely powerful, reducing the accuracy of a PAT-trained classifier on ImageNet-100 to 2.0% when using the high bound of $\epsilon = 1$ from Table 4.

Besides these experiments, we always use externally-bounded attacks with AlexNet for evaluation. AlexNet correlates with human perception of adversarial examples (Figure 4) and provides a standard measure of LPIPS distance; in contrast, self-bounded attacks by definition have varying bounds across evaluated models.

Table 5: Accuracy of a PAT-trained ResNet-50 on ImageNet-100 against various perceptual adversarial attacks. PPGD and LPA attacks are shown self-bounded and externally-bounded with AlexNet. We also experimented with two different perceptual projection methods (see Appendix A.4). Bounds are $\epsilon = 0.5$ for self-bounded attacks and $\epsilon = 1$ for externally-bounded attacks, since the LPIPS distance from AlexNet tends to be about twice as high as that from ResNet-50.

Attack	LPIPS model	Projection	Accuracy against PAT
PPGD	self	bisection method	60.8
PPGD	self	Newton’s method	62.1
PPGD	AlexNet	bisection method	55.7
PPGD	AlexNet	Newton’s method	50.5
LPA	self	bisection method	58.4
LPA	self	Newton’s method	59.0
LPA	AlexNet	bisection method	2.0
LPA	AlexNet	Newton’s method	0.4

E PAT Ablation Study

We perform an ablation study of Perceptual Adversarial Training (PAT). First, we examine Fast-LPA, the training attack. We attempt training without step size (η) decay and/or without increasing λ during Fast-LPA, and find that PAT performs best with both η decay and λ increase. Second, we also compare attacking every input with Fast-LPA during training to only attacking the natural inputs which are already classified correctly. We find that the latter method achieves higher natural accuracy at the cost of some robust accuracy.

Table 6: Accuracies against various attacks for models in the PAT ablation study. Attack bounds are $8/255$ for L_∞ , 1 for L_2 , 0.5 for PPGD/LPA, and the original bounds for StAdv/ReColorAdv.

Training	Ablation	Attack						
		None	L_∞	L_2	StAdv	ReColorAdv	PPGD	LPA
PAT		81.9	42.3	47.2	51.7	75.4	26.5	5.8
PAT	no η decay	83.2	43.8	48.9	38.9	73.9	28.7	3.0
PAT	no λ increase	85.8	38.6	41.2	30.6	72.6	24.7	2.1
PAT	no η decay or λ increase	83.7	41.4	46.7	39.6	73.6	26.3	2.0
PAT	attack all inputs	72.8	44.0	47.9	60.4	68.3	32.8	6.6

F Experiment Details

For all experiments, we train ResNet-50 [34] with SGD for 100 epochs. We use 10 attack iterations for training and 200 for testing, except for PPGD and LPA, where we use 40 for testing since they are more expensive. Self-bounded PAT takes about 12 hours to train for CIFAR-10 on an Nvidia RTX 2080 Ti GPU, and about 5 days to train for ImageNet-100 on 4 GPUs.

We implement PPGD, LPA, and PAT using PyTorch [43]. For L_p adversarially trained models on CIFAR-10, we use pretrained models from the robustness library [44]. For UAR attack adversarially trained models on ImageNet-100, we use the pretrained models from Kang et al. [18].

We preprocess images after adversarial perturbation, but before classification, by standardizing them based on the mean and standard deviation of each channel for all images in the dataset. We use the default data augmentation techniques from the robustness library [44]. The CIFAR-10 dataset can be obtained from <https://www.cs.toronto.edu/~kriz/cifar.html>. The ImageNet-100 dataset is a subset of the ImageNet Large Scale Visual Recognition Challenge (2012) [37] including only every tenth class by WordNet ID order. It can be obtained from <http://www.image-net.org/download-images>.

Table 7: Hyperparameters for the adversarial training experiments on CIFAR-10 and ImageNet-100. For CIFAR-10, hyperparameters are similar to those used by Zhang et al. [7]. For ImageNet-100, hyperparameters are similar to those used by Kang et al. [18].

Parameter	CIFAR-10	ImageNet-100
Architecture	ResNet-50	ResNet-50
Number of parameters	23,520,842	23,712,932
Optimizer	SGD	SGD
Momentum	0.9	0.9
Weight decay	2×10^{-4}	10^{-4}
Batch size	50	128
Training epochs	100	90
Initial learning rate	0.1	0.1
Learning rate drop epochs ($\times 0.1$ drop)	75, 90	30, 60, 80
Attack iterations (train)	10	10
Attack iterations (test)	200	200

F.1 Untargeted and randomly targeted attacks

On CIFAR-10, all evaluations use untargeted attacks; that is, the attack may perturb an input such that is classified as any class except the correct one.

On ImageNet-100, we compare against pretrained models from Kang et al. [18]. They perform training and evaluation using randomly targeted attacks. In these attacks, a target class is randomly chosen from all incorrect classes for each input. Then, the attack only succeeds if it perturbs the input such that it is classified as the specific target class. For a fair comparison, in all ImageNet-100 evaluations we use randomly targeted attacks.

F.2 Layers for LPIPS Calculation

Calculating the LPIPS distance using a neural network classifier $g(\cdot)$ requires choosing layers whose normalized, flattened activations $\phi(\cdot)$ should be compared between images. For AlexNet and VGG-16, we use the same layers to calculate LPIPS distance as do Zhang et al. [22]. For AlexNet [35], we use the activations after each of the first five ReLU functions. For VGG-16 [36], we use the activations directly before the five max pooling layers. In ResNet-50, we use the outputs of the conv2_x, conv3_x, conv4_x, and conv5_x layers, as listed in Table 1 of He et al. [34].